JOURNAL OF MATERIALS SCIENCE 29(1994) 5664–5672

Production of ultrafine alpha alumina powders and fabrication of fine grained strong ceramics

S. RAJENDRAN*
Advanced Materials Program, Australian Nuclear Science and Technology Organisation, Private Mail Bag 1, Menai, NSW 2234, Australia

Hydrous alumina powders, pure, seeded with alpha alumina, containing ammonium nitrate and containing both ammonium nitrate and seeds, were prepared by hydroxide precipitation. Their crystallization and sintering behaviour were investigated and mechanical properties of the ceramics were tested. Pure hydrous alumina transformed to alpha alumina crystals, with a size of ca. 200 nm, at 1200 °C, after undergoing the usual metastable phase changes during heat-treatment. The powder needed to be sintered at 1600 °C to achieve a high density. The ceramic had an average grain size of ca. 9 μm. Seeding lowered the transformation temperature to ca. 1120 °C and caused the transformation to begin at ca. 600 °C. The material could be sintered at 1500 °C and had a grain size of 2 μm. The nitrate, predominantly present as ammonium nitrate, lowered the transformation temperature to ca. 1150 °C and altered the proportion of the intermediate phases. However, the materials still had to be sintered at 1500 °C to achieve > 97% density. When both seed particles and nitrate ions were present the material almost completely transformed at 950 °C to uniform crystals of alpha alumina with a size < 60 nm that sintered to > 99% theoretical density at 1450 °C. The final ceramic had a uniformly grained (< 1.0 μm) microstructure and exhibited strength up to 800 MPa.

1. Introduction

Properties of ceramics depend very much on the final sintered microstructures. Therefore, they have to be tailored carefully to fabricate ceramics with desired properties. However, the microstructural development of a ceramic, during firing, depends on the characteristics of the powders used [1–3]. It is essential to use powders of carefully controlled characteristics for the fabrication of ceramics with controlled microstructures.

A number of wet chemical methods have been developed over the years for the production of single and multi-component oxides [4–7] which allow a very fine and reactive powder to be prepared, and the powder characteristics can be easily modified by changing the conditions during powder synthesis. However, to produce stable crystalline compounds that are suitable for ceramic processing the chemically derived precursors have to be calcined at high temperatures. For instance, hydrous aluminas produced by wet chemical methods have to be calcined at > 1200 °C [8, 9] to crystallize alpha alumina. The resulting powders are, in general, composed of strongly bonded aggregates with relatively larger crystals that require many hours of milling and sintering aids to fabricate relatively dense ceramics with reasonable properties.

It has been reported that the alpha alumina transformation temperature can be reduced to ca. 1050 °C by seeding transition aluminas, such as boehmite with fine epitaxial particles, like alpha alumina and haematite [8–11]. Alpha alumina powder produced by a sol–gel technique [9, 10], which involved the use of seeds, has been reported to sinter readily to near theoretical density at moderate temperatures.

The seeding technique was incorporated into a simple precipitation method to produce reactive alpha alumina powder. However, during the course of the study it became apparent that certain anions together with seeds facilitated the production of fine alpha alumina powder [12–14]. In this paper the crystallization behaviour of four hydrous aluminas prepared by a precipitation method is reported. Sintering characteristics of the powders of the ceramics produced are discussed, as are the microstructures and mechanical properties of a few of the ceramics.

2. Experimental procedure

Four hydrous alumina powders, unseeded nitrate free (AL), seeded (5% alpha alumina seed) nitrate free (ALS), unseeded nitrated (45% ammonium nitrate) (ALN) and seeded nitrated (5% seed and 45% ammonium nitrate) (ALSN), were prepared by a hydroxide precipitation method.

The hydrous alumina powders were prepared by adding an aluminium nitrate solution (0.2 mol dm^{-3}) to a rapidly stirred ammonia solution. The slurry pH

* *Present Address*: Ceramic Fuel Cells Limited, 710 Blackburn Road, Clayton, Victoria 3168, Australia.

0022–2461

was adjusted to ca. 9.0 and stirring continued for another 60 min. The slurry was then filtered and the filter cake divided into two portions. One portion (AL) was washed repeatedly (10–12 times) with deionized water, while the other portion was kept without washing (ALN). Both powders were then dried in an air oven at 110 °C for 24 h. Similarly, the seed was initially mixed with the aluminium nitrate solution and the above processing repeated (powders ALS and ALSN, respectively). The amount of nitrate present in the powders was analysed by ion chromatography (Dionex 4500i). Powders AL and ALS had no detectable nitrate present (< 100 p.p.m) while powders ALN and ALSN contained ca. 45 wt % ammonium nitrate (on an alumina basis).

The powders were calcined at several selected temperatures between 110 and 1200 °C for 1 h and characterized by differential thermal analysis (DTA; Setaram TAG 2400), X-ray diffraction (XRD; Siemens Kristalloflex diffractometer with CoK_α radiation) and transmission electron microscopy (TEM; Jeol FX 2000).

Oxide powders, prepared by calcining the precursor powders between 950 and 1200 °C, were cold-pressed into bars at 200 MPa pressure and sintered between 1200 and 1600 °C for 2 h. Bulk densities of the sintered bodies were determined by mercury displacement. Microstructures of the polished and thermally etched sintered ceramics were analysed using scanning electron microscopy (SEM). Three-point bend fracture strength measurements were made using an Instron 1122 (M/C No. 13) with an outer span of 25 mm and a crosshead speed of 0.05 mm min^{-1}. Fracture toughness measurements were made by the indentation method using 10 and 5 kg loads.

3. Results and discussion

3.1. Powder characterization

3.1.1. Differential thermal analysis (DTA)

DTA curves of all the specimens had three endothermic peaks at 110, 260 and 420 °C, which were associated with a considerable amount of weight loss. The endotherms are assigned to the removal of adsorbed water, and the decomposition of hydroxide and oxy-hydroxide of aluminium, respectively [13]. In addition to those peaks, powders ALN and ALSN had a very sharp exothermic peak at 320 °C due to the decomposition of nitrate present in the material. The DTA curves also showed an exothermic peak at higher temperatures due to the crystallization of alpha alumina. Powder AL had its exothermic peak at 1220 °C, whereas powders ALS, ALN and ALSN showed the peak at 1118, 1155 and 1009 °C, respectively (Table I).

3.1.2. X-ray diffraction (XRD)

The XRD pattern of AL-200 (AL calcined at 200 °C) consisted of at least three phases, well-crystallized aluminium hydroxides (bayerite and nordstrandite) and an amorphous phase (Fig. 1). At 350 °C (AL-350), the aluminium hydroxide peaks disappeared and those corresponding to boehmite (AlOOH) and gamma alumina appeared. Material calcined at 450 and 650 °C (AL-450 and AL-650) gave diffraction peaks due to gamma and delta alumina, while the peaks for delta and theta alumina occurred in the patterns of AL-800 and AL-900. At 1000 and 1100 °C only theta alumina was observed and at 1200 °C the peaks corresponded to alpha alumina crystals.

Calcined ALS powders gave XRD patterns similar to those obtained from AL. The only exception was that all patterns of the ALS powder had alpha alumina peaks, initially due to the seeds, whose intensity increased with increasing calcination temperature above 600 °C. Material calcined at 1000 and 1050 °C (ALS-1000 and ALS-1050) showed only theta and alpha alumina. Small amounts of residual theta alumina were still present in ALS-1100.

The nitrated (ALN) and seeded/nitrated (ALSN) hydrous alumina powders initially showed the patterns for crystalline ammonium nitrate. They behaved quite differently during subsequent heat-treatment

TABLE I Effect of seeding and/or nitrate on the transformation temperature of alpha alumina

Powder (°C)	Alpha alumina transformation temperature	
	DTA	XRD
AL	1220	1150–1200
ALS	1118	600–1100
ALN	1155	1050–1150
ALSN	1009	775–950

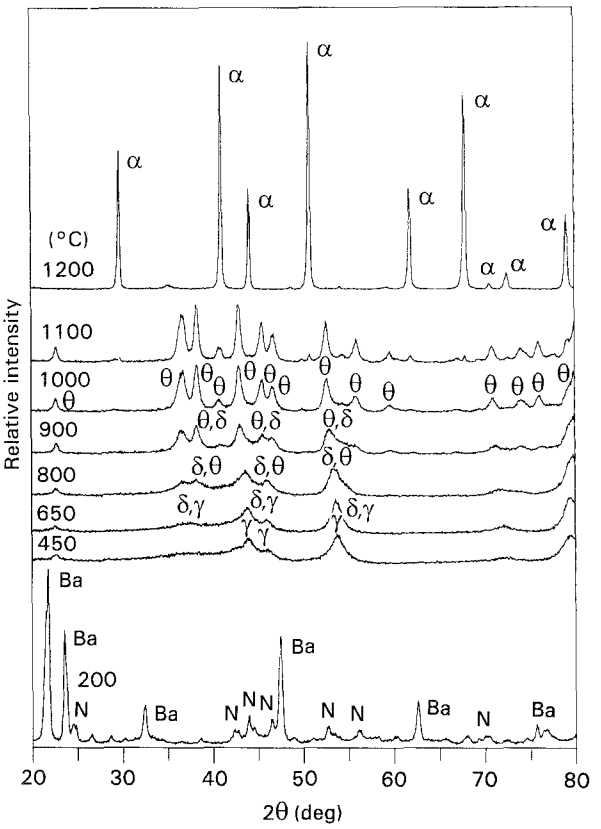

Figure 1 Powder XRD patterns of pure hydrous alumina (AL) calcined at different temperatures. Ba, bayerite; N, nordstrandite; Bo, Boehmite; γ, gamma alumina; δ, delta alumina; θ, theta alumina; α, alpha alumina.

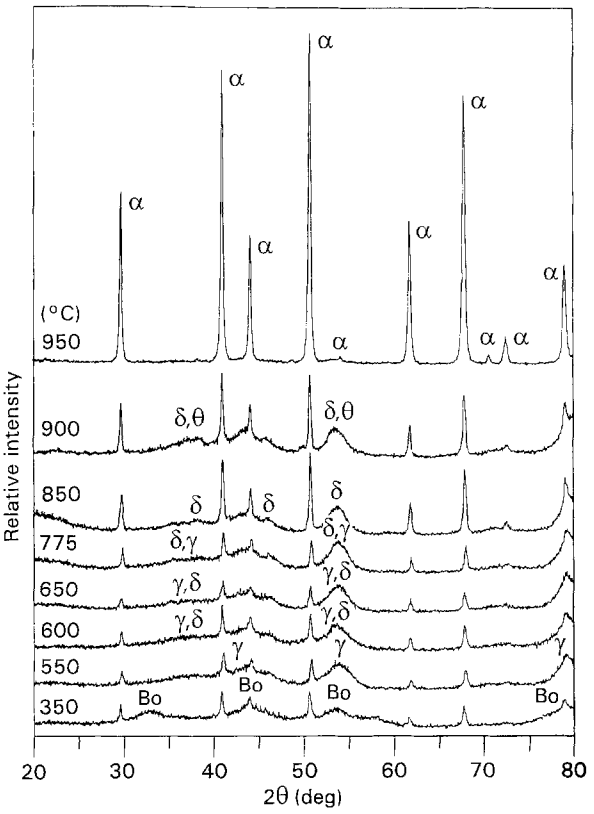

Figure 2 Powder XRD patterns of nitrated/seeded hydrous alumina powder (ALSN) calcined at different temperatures. Ba, bayerite; N, nordstrandite; Bo, Boehmite; γ, gamma alumina; δ, delta alumina; θ, theta alumina; α, alpha alumina.

when compared with AL and ALS. There were sharp peaks in the patterns of powder ALSN calcined below 600 °C due to the alpha alumina seed particles (Fig. 2). When calcined at 350 °C, both powders had very broad peaks in the positions expected for boehmite, indicating that the material was either amorphous or cryptocrystalline. ALN-650 and ALSN-650 patterns mainly corresponded to the peaks for gamma alumina, while delta alumina peaks were also present in the patterns of the materials calcined between 775 and 900 °C. Only very minor amounts of theta alumina were present in any of these powders, as the predominant peaks for the phase were almost absent in the XRD patterns. The gamma and delta alumina peaks were broader (Fig. 2) than the corresponding peaks in the AL and ALS XRD patterns. This suggests that either the atoms were arranged in a disorderly manner in the unit cell of these phases in the calcined ALN and ALSN, or that they had much smaller crystallite sizes. However, TEM results (Section 3.1.3) showed that all the transition aluminas had very fine crystallites (< 10 nm), so it is unlikely that the increased broadening observed in these peaks was due to dramatic changes in the crystallite size [13].

3.1.3. Transmission electron microscopy (TEM)

TEM investigations of the powder AL-200 showed that the major component of the powder consisted of porous, spongy plates of irregular shapes in the size range of 100–2000 nm (Fig. 3a). Electron diffraction patterns from such fragments contained very diffuse, hardly detectable haloes, or a set of weak diffuse rings with spacings consistent with those from aluminium hydroxides. In addition, the TEM images of the powders showed the presence of relatively large, well-formed rectangular crystals (ca. 1000 nm in size) of bayerite.

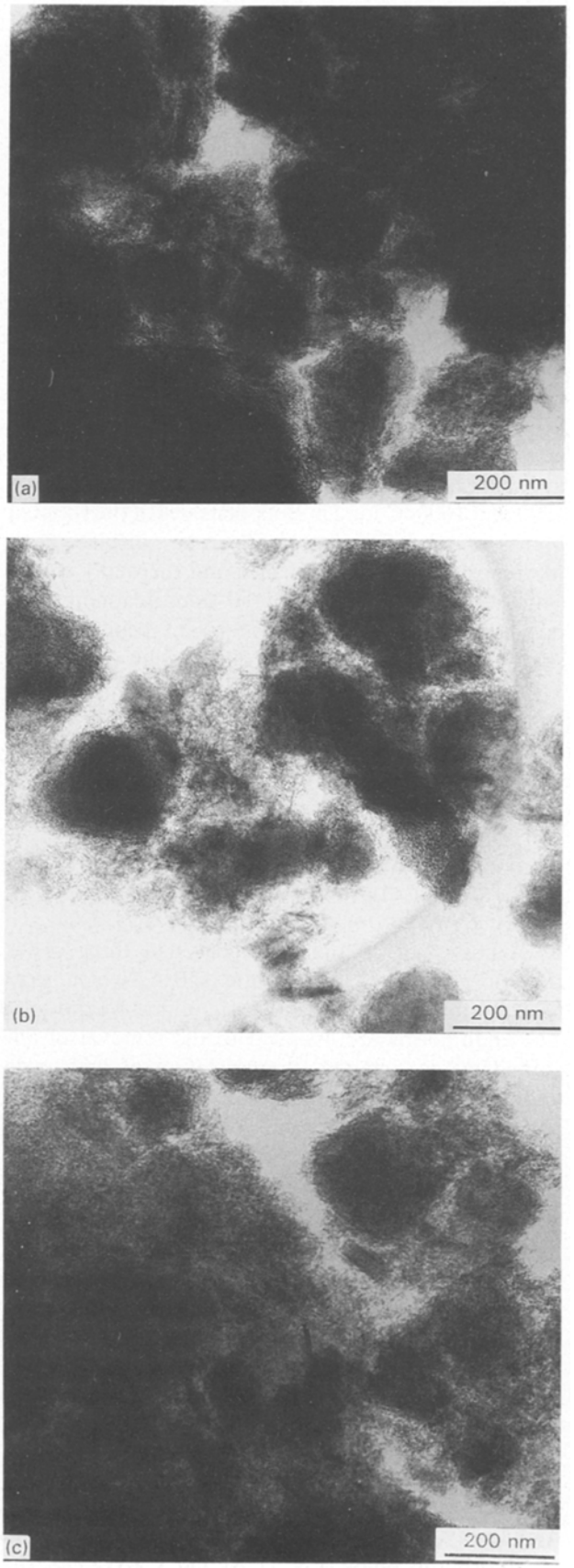

Figure 3 TEMs of AL heat-treated for 1 h at different temperatures (°C): (a) 200; (b) 400; (c) 600; (d) 800; (e) 1000; (f) 1200.

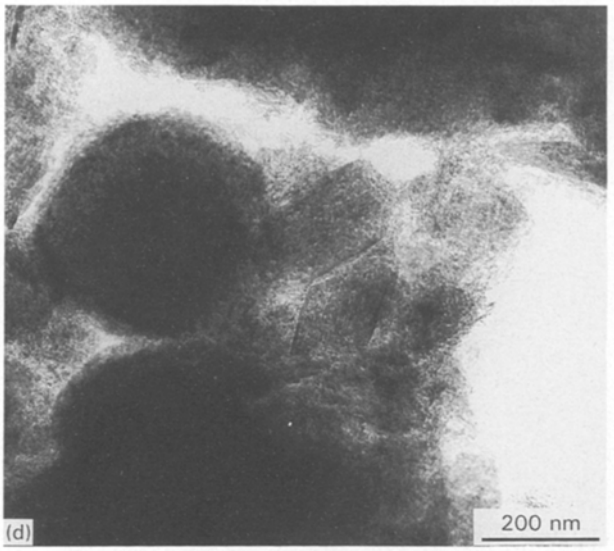

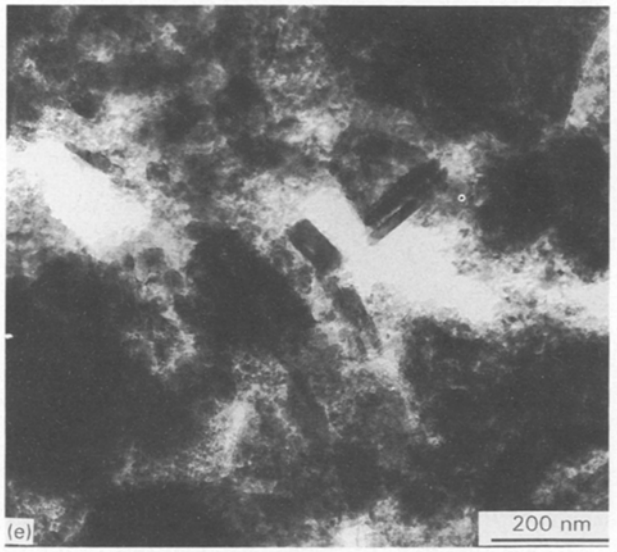

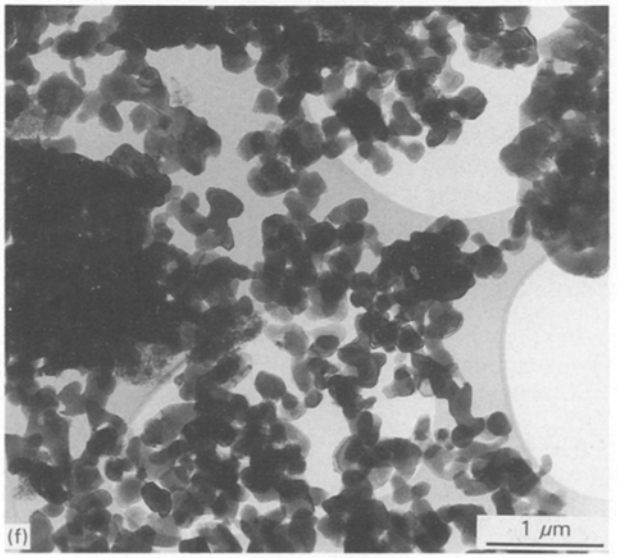

Figure 3 (continued).

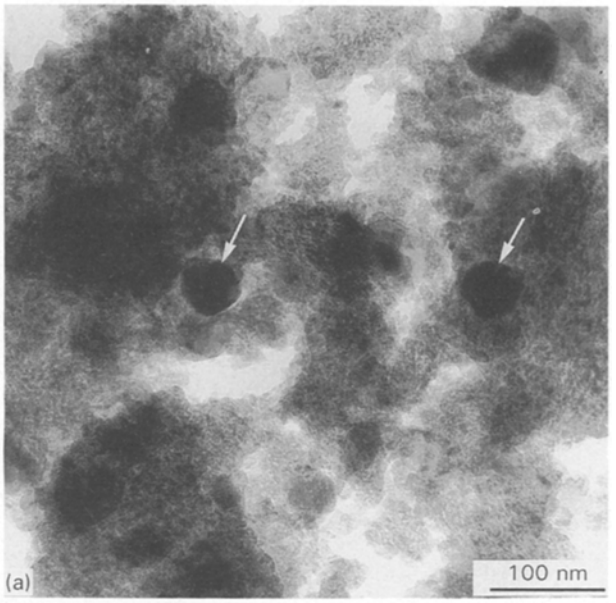

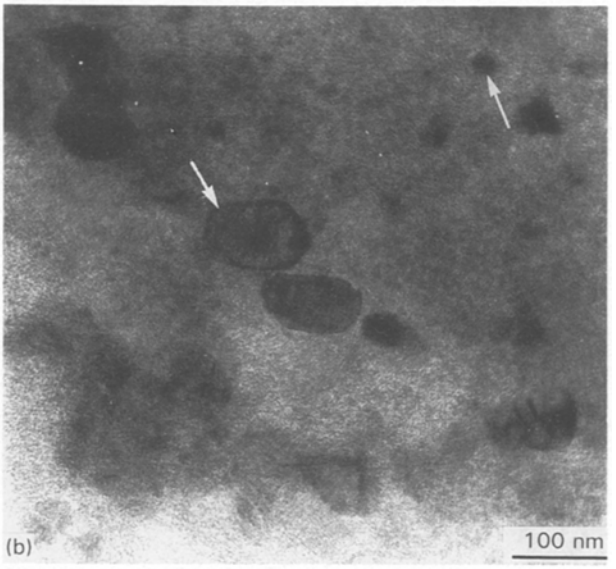

Figure 4 TEM images of hydrous alumina calcined at 350 °C for 1 h. (a) Powder ALS; (b) powder ALSN.

The morphology of the powders was unchanged with increasing calcination temperatures up to 1000 °C (Fig. 3b–e). The appearance of the porous fragments was similar to those observed in AL-200. However, the crystallinity of the fragments increased with increasing calcination temperature. The morphology of the fragments changed markedly after calcination at 1200 °C for 1 h and the material consisted of polycrystalline aggregates with a crystallite size of ca. 200 nm (Fig. 3f). The electron diffraction patterns showed sharp spots, consistent with the *d*-spacings expected for alpha alumina.

The TEMs of powders ALS, ALN and ALSN heat-treated up to 900 °C showed fragments that were quite similar in morphology to those observed in the calcined powders of AL. The fragments present in the specimens of ALS and ALSN contained embedded angular crystals of alpha alumina (Fig. 4), the proportion of which increased with increasing calcination temperature (Fig. 5). Their presence is shown by spots in the diffraction patterns, and their distribution can be seen in the dark field images formed from beams corresponding to such spots (Fig. 6). The morphology of the materials again changed markedly after heat-treatment of the powders at higher temperatures. The

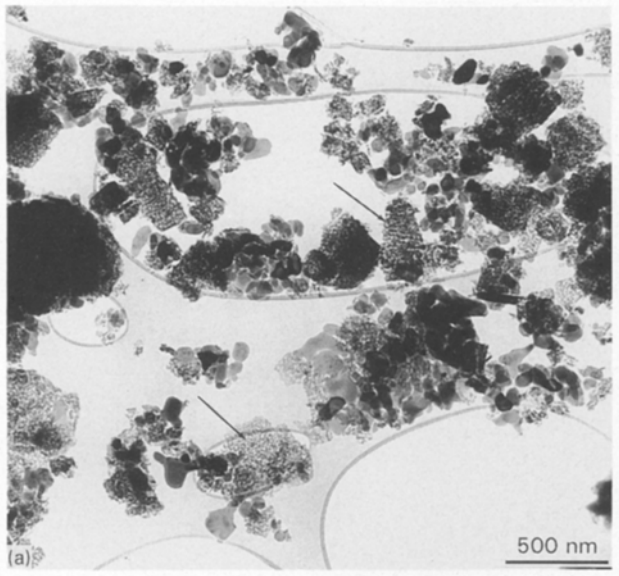

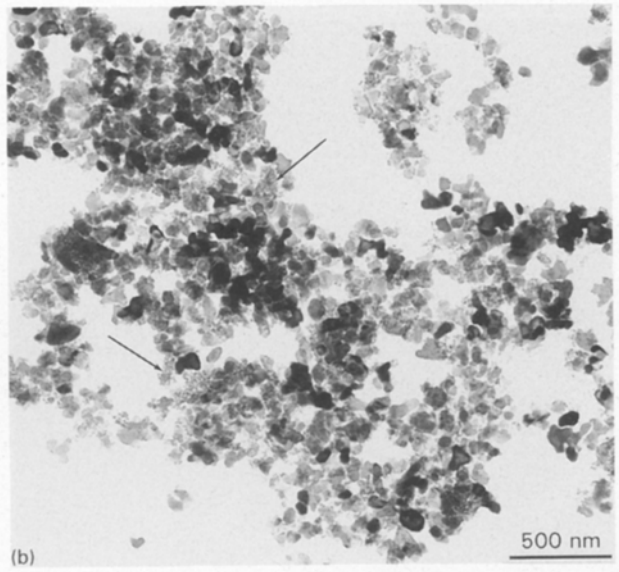

Figure 5 TEMs of ALS calcined for 1 h at (a) 1000 °C; (b) 1100 °C.

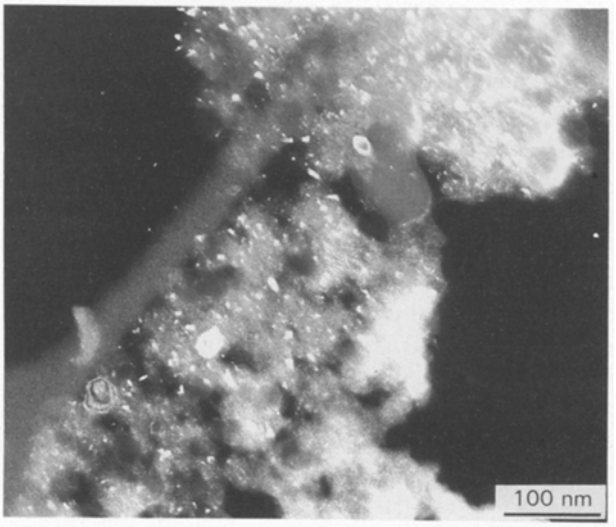

Figure 6 Dark-field TEM image of powder ALSN calcined at 850 °C for 1 h. The size and distribution of alpha alumina crystals within the transition alumina fragments can be seen as bright areas scattered uniformly throughout the fragments.

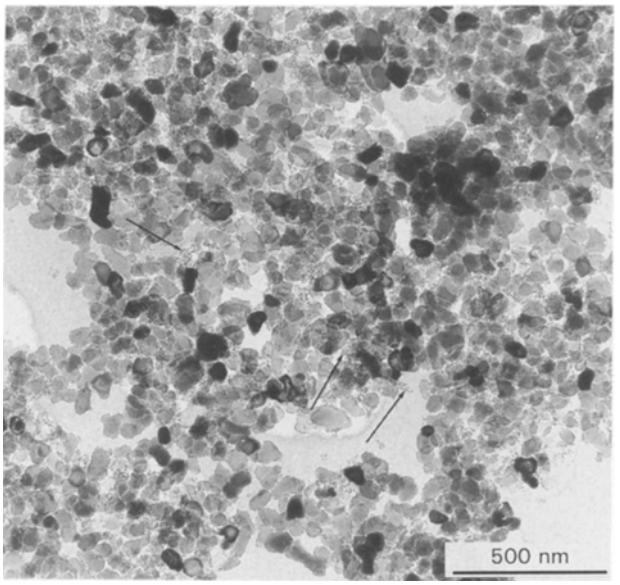

Figure 7 TEM image of ALSN powder heat-treated at 950 °C for 1 h. The theta alumina crystals present in the micrograph are arrowed.

ALSN-950 powder appeared to be homogeneous and consisted mainly of polycrystalline material with a crystallite size of ca. 60 nm (Fig. 7) with a small amount (< 5%) of extremely fine (size < 10 nm, arrowed in the images) crystallites. Diffraction from the finer crystals gave ring patterns corresponding to the intense reflections of theta alumina, while the relatively larger crystals gave sharp diffraction spots consistent with those of alpha alumina (Fig. 8).

During thermal treatment, the hydrous alumina transformed to several metastable transition aluminas before ultimately converting to stable corundum crystals [15, 16]. The transformation sequence and the temperature at which different phases are formed during heat-treatment will be determined by the chemical composition and the structure of the initially formed species. The XRD and TEM analyses of the calcined powders revealed that both AL and ALS undergo the following types of transformation during calcination:

$$\text{Hydrous alumina} \xrightarrow{-XH_2O} \text{Boehmite} \xrightarrow{-H_2O} \text{Gamma} \longrightarrow \text{Delta} \longrightarrow \text{theta} \longrightarrow \text{alpha alumina}$$

The fact that both AL and ALS undergo a similar transformation sequence during heat-treatment indicates that the seed particles in the powder ALS did not alter the primary particle formation during precipitation or their structure in any significant way. However, the crystallization of alpha alumina occurred at a lower temperature (Table I) for ALS, showing that the seeds in the powder acted as nucleation sites. Seeds, when present in a sufficient amount, have been reported to reduce the theta to alpha alumina conversion temperature because they reduce the activation energy barrier involved in the thermally activated nucleation process [10, 11].

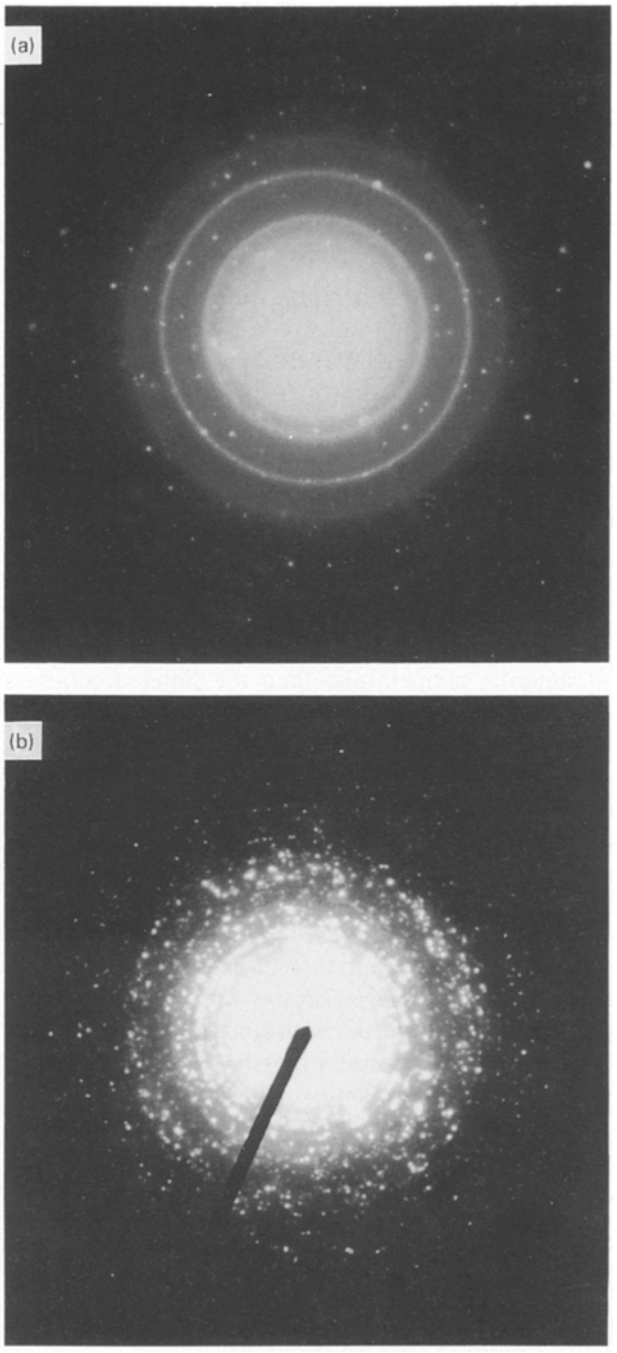

Figure 8 Electron diffraction patterns of ALS powder calcined at 1000 °C for 1 h. (a) From areas of finer crystals; (b) from areas of larger crystals.

The thermal characteristics of powders ALN and ALSN can be explained by considering the influence of ammonium nitrate present in the materials. The effect of nitrate ions in reducing the transformation temperature has been explained in detail elsewhere [13] and is only briefly mentioned here. During calcination the ammonium nitrate decomposes with release of a large amount of energy (210 KJ mol^{-1} [17]) and oxides of nitrogen and nitric acid (by the reaction of oxides of nitrogen with the hydroxyl ions of hydrous alumina) evolve from the powder at 320 °C. The reaction and the evolution of a large amount of energy might:

1. Introduce a considerable amount of high energy defects in the transition alumina matrix. When destroyed, partially or fully, these defects will release energy which can contribute to the energy needed to overcome the activation energy barrier for nucleation of alpha alumina [13, 18].
2. Induce the transformation of some amount of transition alumina to alpha at a relatively low temperature and therefore the nitrate containing material will always have a few extra alpha alumina nuclei than those of AL and ALS (differences in nucleation density [19]) which can help reduce the transformation temperature.
3. Destroy the normal arrangement of atoms, producing a highly disordered structure in the lattices of the boehmite and other transition alumina phases (Fig. 2). These disordered intermediate, metastable phases will transform to the stable corundum structure when minimum, but sufficient, energy is given to the system [13].

3.2. Sintering behaviour, microstructures and mechanical properties of the materials

3.2.1. Sintering characteristics

Pore size distributions of the iso-pressed green compacts are given in Fig. 9 and the other microstructural features of the compacts are presented in Table II. The most frequent pores appear at 130, 36, 57 and 26 nm for the compacts AL, ALS, ALN and ALSN, respectively. The compact ALS has a small amount of second pore population in the 10–20 nm range which prob-

TABLE II Calcination temperature and surface area of the powders and the microstructures of the corresponding green bodies

Properties	Materials			
	AL	ALS	ALN	ALSN
Calcination temperature (°C)	1200	1100	1100	950
Phase analysis	Alpha	Alpha + > 5% theta	Alpha	Alpha + < 5% theta
Surface area ($m^2 g^{-1}$)	8.4	21.9	12.2	35
Average crystallite size (nm)				
(a) TEM	200	90	120	60
(b) Surface area[a]	180	69	124	43
Green Density (% TD)	46	40	58	47
Most frequent pore size (nm)	130	57	36	26
Open pore volume (ml g^{-1})	0.324	0.300	0.214	0.265

[a] Calculated assuming spherical crystallites.

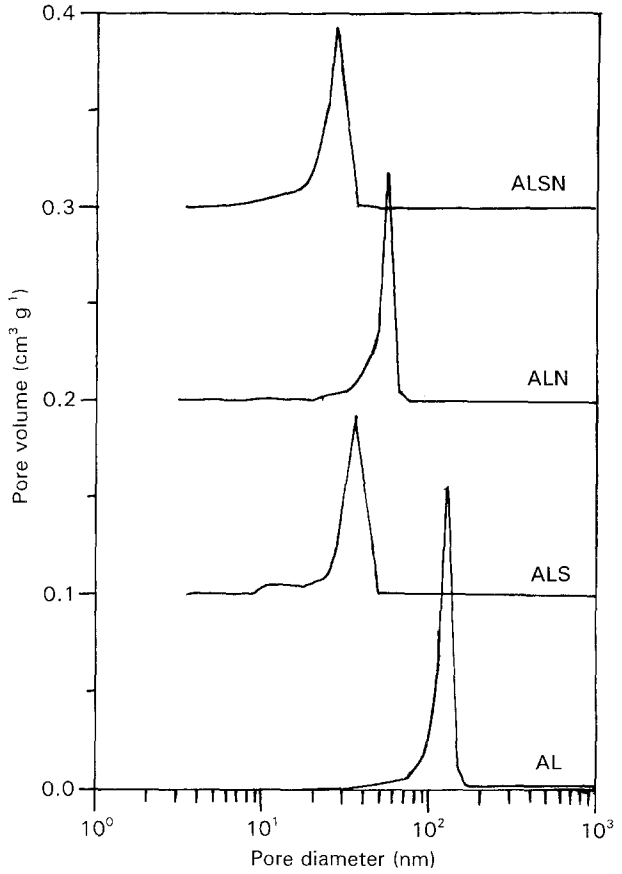

Figure 9 Pore size frequency distribution of iso-pressed green compacts of powders AL, ALS, ALN and ALSN.

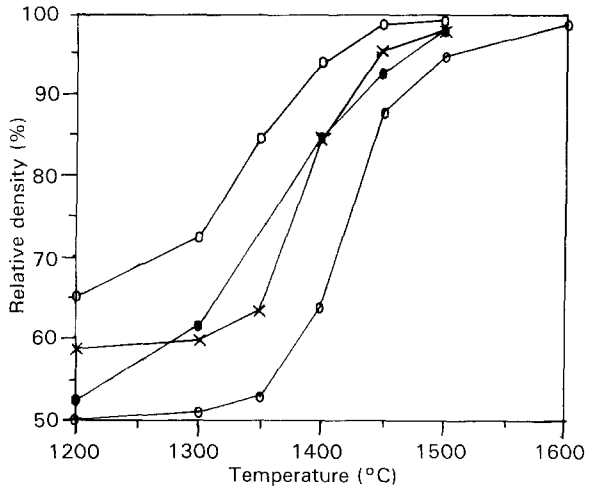

Figure 10 Bulk density (expressed as % TD) of AL (⊖—⊖), ALS (●), ALN (×) and ALSN (○–○) sintered at 1200–1600 °C for 2 h.

ably relates to the residual theta alumina present in the powder. The smaller pore size distribution for ALSN compared to other materials suggests that it compacted uniformly. The powder was composed of soft agglomerates with fine particles (Fig. 7) which could pack uniformly with a narrow pore size distribution during compaction.

Bulk density [expressed as the percentage of theoretical density (TD)] of the materials sintered between 1200 and 1600 °C is shown in Fig. 10. AL started to sinter only above 1300 °C and the material needed to be sintered at 1600 °C to achieve about 98% TD. On the contrary, ALSN commenced sintering as low as 1000 °C and attained ca. 99% TD when sintered at 1450 °C for 2 h. The sinterability of ALS and ALN was moderate: these materials had sinterability better than AL but worse than that of ALSN. Both ALS and ALN reached ca. 97% TD when sintered at 1500 °C.

3.2.2. Microstructure and mechanical property results

SEMs of AL sintered at 1450 and 1500 °C, and ALS and ALSN sintered at 1450 °C for 2 h are given in Fig. 11. SEM images of AL show uneven grain growth (areas of larger and smaller grains) and discontinuous grain growth. The sintered ceramics also had areas of dense and less sintered regions (Fig. 11a and b). The material sintered at 1450 °C had an average grain size of ca. 1.8 μm, which increased to 3.5 and 9.0 μm after sintering at 1500 and 1600 °C, respectively. ALS and ALSN exhibited normal grain growth with an increase in sintering temperatures, and the sintered ceramics had relatively uniform microstructures (smaller grains with narrow size distribution, Fig. 11c and d). Grain size analysis, using the linear intercept method, showed an average grain size of 0.94 μm for ALSN sintered at 1450 °C, which increased to ca. 1.40 μm after sintering at 1500 °C.

Fracture strength and toughness results of AL and ALSN sintered at different temperatures are given in Table III. These results are discussed in detail elsewhere [20], but some features are relevant for the correlation of properties with sintered ceramic microstructures. The fracture strengths exhibited by these materials were significantly higher than those reported for conventionally milled and sintered aluminas [21]. The material sintered between 1450 and 1500 °C had a fracture strength > 750 MPa, with a toughness of 5.5 MPa $m^{1/2}$, both of which are much higher than the values exhibited by AL. The improvement in the properties of ALSN compared to AL can be related to differences in the microstructures of the ceramics fabricated from the two powders.

The differences in the sinterability of the materials and the resultant ceramic microstructures can be explained by considering the characteristics of the powders and the compacted green bodies (Figs 3f, 5b, 7 and 9, Table II). ALS and ALSN contained relatively fine weakly aggregated crystallites which packed uniformly with a narrow pore size distribution compared to AL and ALN. The latter powders were composed of relatively strong aggregates (necking can be seen in Fig. 3f). However, the sinterability of ALS was less than that of ALSN because the residual theta alumina, which transformed to alpha only at 1200 °C or above, controlled the sinteractivity of the material. The finer alpha alumina crystals in ALN packed uniformly with smaller pores and hence sintered faster than AL.

The kinetics of densification and grain growth are closely related [22]. In the early stages of sintering grains grew almost linearly with densification, but grain growth was very rapid once the density of the compact reached > 90% TD [23]. However, the

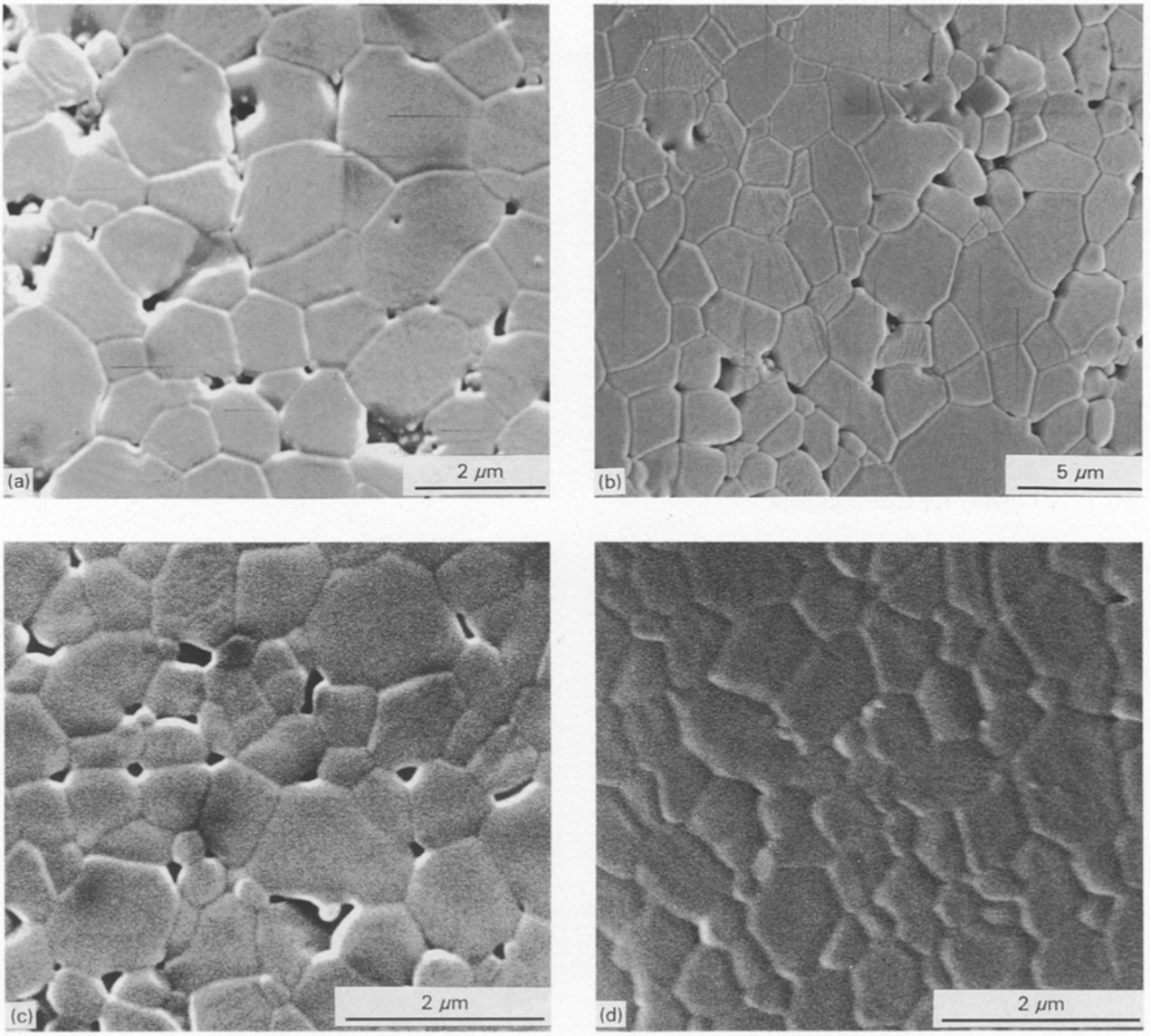

Figure 11 SEMs of materials sintered for 2 h (a) AL-1450 °C; (b) AL-1500 °C; (c) ALS-1450 °C; (d) ALSN-1450 °C.

TABLE III Relative density (% TD), fracture strength (σ, MPa), fracture toughness (K_{1C}, MPa $m^{1/2}$) and average grain size (GS, μm) of AL and ALSN alumina powders sintered at different temperatures for 2 h

Sintering temp. (°C)	Properties of AL				Properties of ALSN			
	σ	K_{1C}	% TD	GS	σ	K_{1C}	% TD	GS
1400	–	–	–	–	475	5.3	93.4	0.79
1450	280	–	88.0	1.8	729	5.5	98.7	0.95
1500	320	–	94.6	3.6	797	5.5	99.2	1.20
1600	460	3.7	98.4	9.0	–	–	–	–

amount of grain growth required for the achievement of full density depends on the pore coordination number (n; pore surrounded by number of grains). If $n < n_c$ (critical coordination number) then the grain growth needed for full densification is small [24]. ALSN had an average pore size of ca. 26 nm, i.e. almost five times smaller than the average pore channels of the compact AL (Fig. 9). Accordingly, the amount of grain growth needed for AL is high.

4. Conclusions

1. Pure hydrous alumina (AL) transformed to corundum crystals at ca. 1200 °C. The powder was composed of relatively strong, large aggregates and the material required sintering at 1600 °C to fabricate dense ceramics with reasonable fracture properties.

2. Crystallization of alpha alumina occurred at ca. 1100 °C when hydrous alumina contained either alpha alumina seeds (ALS) or nitrate ions (ALN). These

powders reached almost the same density (> 97% TD) when sintered at 1500 °C irrespective of the differences in both powder and compacted green body microstructures.

3. ALSN powder was almost fully converted to alpha alumina at 950 °C. The resulting powder contained soft agglomerates with fine, uniform crystallites which densified to > 99% TD at 1450 °C. The sintered ceramic had a uniformly fine grained microstructure and exhibited relatively high fracture strength and toughness.

Acknowledgements

The author thanks Dr M. J. Bannister, CSIRO, Materials Science and Technology Division, Clayton, Victoria, Australia, for reviewing the manuscript and Mr D. J. Cassidy for technical help.

References

1. E. D. H. HUBNER, Alumina – Processing, properties and applications (Springer-Verlag, New York, 1970).
2. H. K. BOWEN, *Mater. Sci. Engng.* **44** (1980) 1.
3. G. Y. ONADO Jr and L. L. HENCH (editors) "Ceramic processing before firing" (John Wiley, New York, 1978).
4. L. L. HENCH and D. R. ULRICH (eds) "Ultrastructure processing of ceramics, glasses and composites" (Wiley, New York, 1984).
5. G. L. MESSING, J. W. McCAULEY, K. S. (Joe) MAZDIYASNI and R. A. HABER (eds) "Ceramic powder science" (Adv. Ceram. 21, Amer. Ceram. Soc. Inc., Westerville, OH, 1987).
6. C. J. BRINKER, D. E. CLARK and D. R. ULRICH (eds) "Better ceramics through chemistry III", Mater. Res. Soc. Symp. Proc., Vol 121 (*Mater. Res. Soc.*, Pittsburgh, PA, 1988).
7. G. L. MESSING, S. HIRANO and H. HAUSNER (eds) "Ceramic powder science III", Ceramic Trans., Vol 12 (Amer, Ceram. Soc. Inc., Westerville OH, 1990).
8. M. KUMAGAI and G. L. MESSING, *J. Amer. Ceram. Soc.* **67** (1984) C230.
9. Y. SUWA, R. ROY and S.KOMARNENI, *ibid.* **68** (1985) C238.
10. J. L. MCARDLE and G. L. MESSING, *Adv. Ceram. Mater.* **3** (1988) 387.
11. L. PACH, R. ROY and S. KOMARNENI, *J. Mater. Res.* **5** (1990) 278.
12. S. RAJENDRAN and J. L. WOOLFREY, *Key Engng. Mater.* **48–50** (1990) 462.
13. S. RAJENDRAN, D. J. CASSIDY and J. L. WOOLFREY, Unpublished work.
14. S. RAJENDRAN, Unpublished work.
15. K. WEFERS and G. M. BELL, in "Oxides and hydroxides of aluminium" (Technical Paper No. 19, Alcoa Res. Lab., 1972).
16. C. MISRA, "Industrial alumina chemicals" (ACS Monograph 184, Amer. Chem. Soc., Washington, 1986).
17. J. W. MELLOR, "Mellor's comprehensive treatise on inorganic and theoretical chemistry", Vol. 8, Nitrogen Part II (Longman's, London, 1967).
18. G. A. CHADWICK, "Metalography of phase transformations" (Butterworths, London, 1972), p. 194.
19. W. A. YARBROUGH and R. ROY, *J. Mater. Res.* **2** (1987) 494.
20. S. R. WITEK and E. P. BUTLER, *J. Amer. Ceram. Soc.* **69** (1986) 523.
21. S. RAJENDRAN, Unpublished work.
22. C. A. HANDWERKER, R. M. CANNON and R. L. COBLE, "Structure and properties of MgO and Al_2O_3 ceramics, Advances in Ceramics 10", edited by W. D. Kingery (Amer. Ceram, Soc., Columbus, OH, 1984) p. 619.
23. T. K. GUPTA, *J. Amer. Ceram. Soc.* **55** (1972) 276.
24. B. J. KELLETT and F. F. LANGE, *ibid.* **72** (1989) 725.

Received 2 August 1993
and accepted 21 April 1994